A Simple Calibration for Upper Limb Motion Tracking and Reconstruction

Yan Wang, James Xu, Xiaoxu Wu, Gregory Pottie and William Kaiser
Department of Electrical Engineering
University of California, Los Angeles, California 90095
{phylliswany, jyxu, xiaoxuwu}@ucla.edu, {pottie, kaiser}@ee.ucla.edu

Abstract— **This paper extends the work of inertial sensor based upper limb motion tracking by introducing a simple calibration method to automatically construct a global reference frame and estimate arm length. The method has effectively eliminated the requirement of manually aligning the sensors' local reference frames when multiple sensors are used to track the movements of the individual arm segments. The capacity of arm length estimation also makes it possible to reconstruct position trajectories of the elbow and the wrist joints in a reference frame with the shoulder joint as the origin. Verification of the algorithm has been done by comparing the estimated arm length with the Kinect captured pseudo ground truth. Effectiveness of the algorithm can be observed by visualizing the reconstructed position trajectories of the arm joints.**

I. INTRODUCTION

The critical benefits activity monitoring provides in health and wellness promotion, and disease treatment have been widely confirmed [1]. Advances in embedded technology have led to the proliferation of wearable inertial sensor based activity monitoring systems. In [2], a waist-mounted tri-axial accelerometer was used to detect falls and classify lower body transitional movements. In [3], wireless inertial sensors containing accelerometers, gyroscopes, and magnetometers were used to determine foot motions in 3D space.

Compared to lower body activity monitoring, the upper body is more difficult due to a number of complications: 1) increased degrees of freedom of the upper body joints imply that different people can exhibit entirely different motions for the same activity, and within-subject motions may vary for the same activity; 2) the activity may be performed variably depending on physical condition and surroundings; and 3) no strong, identifiable signatures distinguish upper body motions. Therefore, little research has been published on activity classification in the domain of upper body motions except those aimed at classifying a strictly defined activity set [4]. On the other hand, many works have been focused on the tracking of arm movements with two inertial sensors attached on the upper arm and the lower arm respectively [5] [6]. However, those motion tracking algorithms usually require users to align the sensors to each other and with the mounted arm segment, which prevents their implementation in daily life monitoring.

In this paper, a simple calibration method is introduced, which effectively avoids the burden of manually aligning the sensors. In addition, the algorithm automatically estimates the arm length so that position trajectories of the elbow and the wrist joints can be reconstructed without manual measurements. The rest of the paper will be structured as follows: 1) section II-A will review the widely used upper limb motion tracking algorithm; 2) section II-B will introduce the novel calibration method as well as its contribution; and 3) section III will verify the calibration algorithm and illustrate its effect on upper limb motion reconstruction.

II. ALGORITHM

In the section, algorithms for inertial sensor based upper limb motion tracking and reconstruction will be reviewed followed by the introduction of the new calibration method. Before that, notations used to describe the algorithms will be introduced. Most of the variables will have a left superscript, a right superscript and a right subscript. The left superscript indicates the reference frame the variable is calculated. The right superscript indicates the body segment the variable relates to. The right subscript usually represents the time variable. Exceptions will be explained when they arise.

A. Upper Limb Motion Tracking and Reconstruction

One assumption to model upper limb motions is that we characterize the human arm as two rigid segments, the upper arm and the lower arm. Each of the segments can only rotate about its preceding joints, the shoulder joint or the elbow joint. Thus, a double pendulum model can be applied to characterize full-arm motions. Inertial measurement units (IMUs) are attached on each segment to measure 3D acceleration of the upper arm ${}^{s}\mathbf{a}_t^U$ and the lower arm ${}^{s}\mathbf{a}_t^L$, and 3D angular velocity of the upper arm ${}^{s}\boldsymbol{\omega}_t^U$ and the lower arm ${}^{s}\boldsymbol{\omega}_t^L$ in each sensor's local reference frame at time t. By applying integration on the angular velocity with filtering techniques, for example, the Kalman filter and the complimentary filter [6], instantaneous sensor orientation at time t can be calculated relative to the sensor's initial local reference frame when it was first powered on. Quaternions are used to represent the orientation, which is labeled as ${}^{i}\mathbf{q}_t^U$ and ${}^{i}\mathbf{q}_t^L$ each being a four-element row vector. The left superscript i indicates that it is relative to the sensor's initial local reference frame.

To reconstruct upper limb motions, positions of the elbow and the wrist joints at time t, $\mathbf{p}_t^E$, and $\mathbf{p}_t^W$ are tracked,

978-1-4244-7929-0/14/$26.00 ©2014 IEEE

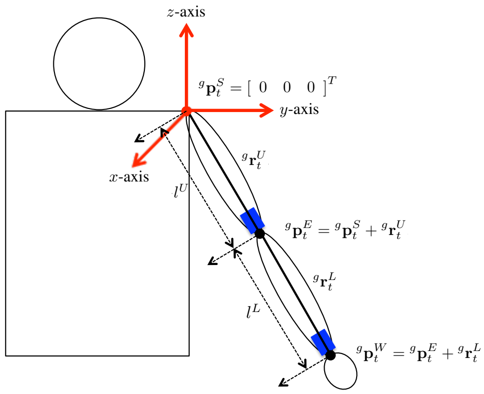

Fig. 1: Double pendulum model to characterize full-arm motions (back view).

neglecting the movements of the shoulder joint. It is essential to have a global reference frame to describe orientations of the upper arm ${}^g\mathbf{q}_t^U$ and the lower arm ${}^g\mathbf{q}_t^L$ so that position trajectories in a uniform global reference frame ${}^g\mathbf{p}_t^E$ and ${}^g\mathbf{p}_t^W$ can be reconstructed. A possible global reference frame can be constructed by setting the x-axis perpendicular to the coronal plane pointing from the chest to the back and the z-axis perpendicular to the axial plane pointing from the feet to the head. Using the right-handed rule, the y-axis can be constructed accordingly. We set the shoulder joint as the origin of the global reference frame where

$${}^g\mathbf{p}_t^S = \left[\begin{array}{ccc} 0 & 0 & 0 \end{array}\right]^T, \tag{1}$$

whose value does not change with the time variable t. Fig. 1 illustrates the global reference frame for upper limb motion reconstruction in the case of the right arm.

When the right arm is straight down at time 0, vectors to characterize the posture of the upper arm and the lower arm are,

$${}^g\mathbf{r}_0^U = \left[\begin{array}{ccc} 0 & 0 & -l^U \end{array}\right]^T, \tag{2}$$

$${}^g\mathbf{r}_0^L = \left[\begin{array}{ccc} 0 & 0 & -l^L \end{array}\right]^T, \tag{3}$$

where l^U and l^L represent the length of the upper arm and the lower arm respectively. By applying the orientation quaternion whose value is $\mathbf{0}$ at time 0 to the two vectors, the posture at time t can be characterized as

$$\left[\begin{array}{c} 0 \\ {}^g\mathbf{r}_t^U \end{array}\right]^T = {}^g\mathbf{q}_t^U \times \left[\begin{array}{c} 0 \\ {}^g\mathbf{r}_0^U \end{array}\right]^T \times \overline{{}^g\mathbf{q}_t^U}, \tag{4}$$

$$\left[\begin{array}{c} 0 \\ {}^g\mathbf{r}_t^L \end{array}\right]^T = {}^g\mathbf{q}_t^L \times \left[\begin{array}{c} 0 \\ {}^g\mathbf{r}_0^L \end{array}\right]^T \times \overline{{}^g\mathbf{q}_t^L}, \tag{5}$$

where $\times$ represents the quaternion product and $\overline{{}^g\mathbf{q}_t^L}$ is the conjugate of ${}^g\mathbf{q}_t^L$. Therefore, position of the elbow and the wrist joints at time t can be calculated as

$${}^g\mathbf{p}_t^E = {}^g\mathbf{p}_t^S + {}^g\mathbf{r}_t^U, \tag{6}$$

$${}^g\mathbf{p}_t^W = {}^g\mathbf{p}_t^E + {}^g\mathbf{r}_t^L. \tag{7}$$

B. Calibration

In the previous section, algorithms to track and reconstruct upper limb motions have been presented. This section will focus on the calibration methods used to 1) construct the global reference frame without requiring sensor alignment to each other or with the mounted arm segment, and 2) create the vectors describing the arm posture at time 0, ${}^g\mathbf{r}_0^U$ and ${}^g\mathbf{r}_0^L$, without measuring the lengths of the arm segments.

Here, a simple calibration procedure is introduced where users are asked to keep their right arm (with the sensors attached on) straight down for a few seconds, for example, from time 0 to time t_1. Then they swing to the side in the coronal plane but still keeping their arm straight and returning to the starting position. The duration can be labeled from time t_1 to time t_2. At the end of the swing, they keep the arm straight down for another few seconds, for example, from time t_2 to time t_3. The only requirement here is that the sensors should be mounted as close to the limb ends as possible. The calibration motion generates two concentric arc-shaped position trajectories of the elbow and the wrist joints in the coronal plane, which can be approximated by the position trajectories of the sensors as they are attached on the limb ends close to the joints.

During the swing, the two sensors are going through a circular motion. Take the sensor on the upper arm close to the elbow joint as an example. Its instantaneous linear and angular velocities in the sensor's local reference frame are related by

$${}^s\mathbf{v}_t^U = {}^s\boldsymbol{\omega}_t^U \times {}^s\mathbf{r}_t^U, \tag{8}$$

where $\times$ here represents the cross product between two three-element column vectors (also applied to Equation (9)) and ${}^s\mathbf{r}_t^U$ is a vector from the rotation center (the shoulder joint) to the sensor described in the sensor's local reference frame. Since the sensor is rotating, so is its local reference frame. Therefore, ${}^s\mathbf{r}_t^U$ must be constant and can be estimated by using the minimum mean square error (MMSE) through the following formula,

$${}^s\mathbf{r}^U = \underset{{}^s\mathbf{r}^U}{\arg\min} \sum_{t=t_1}^{t_2} ||{}^s\boldsymbol{\omega}_t^U \times {}^s\mathbf{r}^U - {}^s\mathbf{v}_t^U||^2. \tag{9}$$

Note that ${}^s\mathbf{r}_t^U$ is replaced by ${}^s\mathbf{r}^U$ as it does not change with the time variable t. Since the cross product between two three-element column vectors can always be reformulated as the product between a matrix and a vector, Equation (9) can be easily solved after being converted to the form of a normal equation.

Though the gyroscope measurements are suffering from continuous drifting after integration, its instantaneous output is reliable. Thus, ${}^s\boldsymbol{\omega}_t^U$ can be directly obtained from the gyroscope measurement. To calculate ${}^s\mathbf{v}_t^U$, the motion tracking algorithm of human gaits [7] is employed. Here a temporary global reference frame is introduced, which is aligned with the sensor's local reference frame when the arm is straight down from time 0 to t_1. Firstly, ${}^i\mathbf{q}_t^U$ is projected to the temporary global reference frame as

$$ {}^{t}\mathbf{q}_t^U = (\overline{{}^{i}\mathbf{q}^U})^{-1} \times {}^{i}\mathbf{q}_t^U, \tag{10} $$

where $\overline{{}^{i}\mathbf{q}^U}$ represents the mean of orientation quaternions from time 0 to t_1. The overscore here as well as in Equation (22) and (23) represent the mean instead of the conjugate. Then, ${}^{s}\mathbf{a}_t^U$ is converted to ${}^{t}\mathbf{a}_t^U$ by using

$$ \begin{bmatrix} 0 \\ {}^{t}\mathbf{a}_t^U \end{bmatrix}^T = {}^{t}\mathbf{q}_t^U \times \begin{bmatrix} 0 \\ {}^{s}\mathbf{a}_t^U \end{bmatrix}^T \times \overline{{}^{t}\mathbf{q}_t^U}. \tag{11} $$

Note that gravity is the only component of the accelerometer measurements in the phase of the arm straight down. Therefore, its vector representation in the temporary global reference frame, ${}^{t}G^U$ can be estimated by averaging ${}^{t}\mathbf{a}_t^U$ from time 0 to t_1. This vector is subtracted from each ${}^{t}\mathbf{a}_t^U$ to remove the gravity component. Then, integration can be performed to calculate the velocity, ${}^{t}\mathbf{v}_t^U$. To reduce integration drifts, zero velocity update (ZUPT) is applied. The zero velocity windows are set to be from time 0 to t_1 and from time t_2 to t_3 corresponding to the two phases of the arm straight down. However, Equation (9) requires the linear velocity in the sensor's local reference frame. Thus, the updated velocity is mapped back through the following formula,

$$ \begin{bmatrix} 0 \\ {}^{s}\mathbf{v}_t^U \end{bmatrix}^T = \overline{{}^{t}\mathbf{q}_t^U} \times \begin{bmatrix} 0 \\ {}^{t}\mathbf{v}_t^U \end{bmatrix}^T \times {}^{t}\mathbf{q}_t^U. \tag{12} $$

By substituting ${}^{s}\boldsymbol{\omega}_t^U$ and ${}^{s}\mathbf{v}_t^U$ into Equation (9), ${}^{s}\mathbf{r}^U$ can be estimated. The same procedure can be applied to calculating ${}^{s}\boldsymbol{\omega}_t^L$ and ${}^{s}\mathbf{v}_t^L$. However, instead of ${}^{s}\mathbf{r}^L$, they are related by ${}^{s}\mathbf{r}^W$, a vector representing the whole arm from the shoulder joint to the wrist joint in the sensor's local reference frame attached on the lower arm. Obviously, the norm of ${}^{s}\mathbf{r}^W$ is larger than that of ${}^{s}\mathbf{r}^U$. Therefore, even without the prior knowledge of the individual sensors' mounting locations, the norm of the rotation radius can be used to infer which sensor is on the upper arm and which is on the lower arm.

Before continuing on the calculation of ${}^{g}\mathbf{r}_0^U$ and ${}^{g}\mathbf{r}_0^L$ based on ${}^{s}\mathbf{r}^U$ and ${}^{s}\mathbf{r}^W$, it is essential to first have the global reference frame mentioned in the previous section. We construct the uniform global reference frame from individual sensors' temporary global reference frames. Take the right upper arm as an example. When the arm is straight down, it is approximately perpendicular to the axial plane. Therefore, $-{}^{t}\mathbf{r}_0^U$ can be set as the z-axis of the global reference frame pointing from the elbow joint to the shoulder joint. Since at time 0, the sensor's local reference frame was aligned with its temporary global reference frame, $-{}^{t}\mathbf{r}_0^U$ is equivalent to $-{}^{s}\mathbf{r}^U$. Meanwhile, since the x-axis is perpendicular to the coronal plane, this can be approximated by finding a vector orthogonal to the swinging plane. The swinging plane is formed by ${}^{t}\mathbf{r}_t^U, t = t_1, ..., t_2$, which can be calculated from

$$ \begin{bmatrix} 0 \\ {}^{t}\mathbf{r}_t^U \end{bmatrix}^T = {}^{t}\mathbf{q}_t^U \times \begin{bmatrix} 0 \\ {}^{s}\mathbf{r}^U \end{bmatrix}^T \times \overline{{}^{t}\mathbf{q}_t^U}. \tag{13} $$

By applying MMSE, the x-axis represented by $\mathbf{x}$ can be obtained by

$$ \mathbf{x} = \arg\min_{\mathbf{x}} \sum_{t=t_1}^{t_2} ||({}^{t}\mathbf{r}_t^U)^T \cdot \mathbf{x}||^2. \tag{14} $$

The remaining y-axis is calculated by the cross product between the z-axis and x-axis. However, in Equation (14), there is no constraint on the direction of the x-axis. To ensure that the it points from the chest to the back, the paired inner product between ${}^{t}\mathbf{r}_t^U$ and the y-axis is calculated. If most of them are negative meaning the swinging plane is along the negative y-axis, directions of the x-axis and y-axis will be flipped. Similar to the visualization frame construction methods in [7], a rotation matrix, R_t^g with its corresponding quaternion representation as $\mathbf{q}_t^g$ can be calculated. Then,

$$ {}^{g}\mathbf{r}_0^U = R_t^g \cdot {}^{t}\mathbf{r}_0^U = R_t^g \cdot {}^{s}\mathbf{r}^U, \tag{15} $$

$$ {}^{g}\mathbf{q}_t^U = \mathbf{q}_t^g \times {}^{t}\mathbf{q}_t^U \times \overline{\mathbf{q}_t^g}. \tag{16} $$

By applying the same algorithm, ${}^{g}\mathbf{r}_0^W$ and ${}^{g}\mathbf{q}_t^L$ can be calculated. Theoretically, ${}^{g}\mathbf{r}_0^W$ and ${}^{g}\mathbf{r}_0^U$ are parallel with their difference equal to ${}^{g}\mathbf{r}_0^L$. Due to sensor noises and estimation errors, ${}^{g}\mathbf{r}_0^L$ is approximated by

$$ {}^{g}\mathbf{r}_0^L = (1 - \frac{||{}^{g}\mathbf{r}_0^U||}{||{}^{g}\mathbf{r}_0^W||}) \cdot {}^{g}\mathbf{r}_0^W. \tag{17} $$

Substituting ${}^{g}\mathbf{r}_0^U$, ${}^{g}\mathbf{q}_t^U$, ${}^{g}\mathbf{r}_0^L$, and ${}^{g}\mathbf{q}_t^L$ into Equation (4), (5), (6), and (7), positions of the elbow and the wrist joints at any time t can be reconstructed.

III. Experiment and Result

Verification of the calibration algorithm is based on accuracy of the arm length estimation. The Invensense MotionFit Boards were used for data collection. The on-board IMU samples the motion data at the rate of 200Hz and the data are transmitted through Bluetooth to a computer for offline processing. 3 females and 5 males with various arm lengths were recruited. Each subject was asked to perform the calibration motion three times with the sensing boards mounted at the end of the upper arm and the lower arm.

Length of the upper arm and the whole arm can be estimated from the calibration procedures through the following formulas,

$$ l_{est}^U = ||{}^{s}\mathbf{r}^U||, \tag{18} $$

$$ l_{est}^W = ||{}^{s}\mathbf{r}^W||, \tag{19} $$

where the right subscripts here no longer represent the time variable. Note that the calibration motions were separated by the zero velocity windows with the posture of arm straight down and the zero velocity windows were detected automatically by thresholding energy of the gyroscope signal.

A Kinect system was set up to capture the skeleton movements at the frame rate of 30Hz. Positions of each body joints including the shoulder joint ${}^{k}\mathbf{p}_t^S$, the elbow joint ${}^{k}\mathbf{p}_t^E$ and the wrist joint ${}^{k}\mathbf{p}_t^W$ in the Kinect's reference frame

TABLE I: Accuracy of Arm Length Estimation

	S1	S2	S3	S4	S5	S6	S7	S8
$\overline{l_{est}^{U}}$ [m]	0.24	0.27	0.23	0.31	0.29	0.27	0.26	0.30
$\overline{l_{est}^{W}}$ [m]	0.45	0.47	0.48	0.59	0.53	0.53	0.51	0.58
e^{U} [%]	5.48	7.36	9.94	3.87	1.07	0.86	4.09	5.17
e^{W} [%]	7.67	2.11	0.65	6.84	0.49	8.07	1.13	6.06

were archived. Based on the rigid segment assumption, we estimate the length of the upper arm as the distance from the shoulder joint to the elbow joint and the length of the whole arm as that from the shoulder joint to the wrist joint during the calibration motion shown in the following formulas,

$$l_{gt}^{U} = \frac{1}{N} \sum_{t=0}^{t_3} ||{}^{k}\mathbf{p}_t^{E} - {}^{k}\mathbf{p}_t^{S}||, \tag{20}$$

$$l_{gt}^{W} = \frac{1}{N} \sum_{t=0}^{t_3} ||{}^{k}\mathbf{p}_t^{W} - {}^{k}\mathbf{p}_t^{S}||, \tag{21}$$

where N is the number of samples between time 0 to t_3. The Kinect data was used as the pseudo ground truth.

The estimated arm length was averaged as well as the pseudo ground truth through the three sets of calibration motions. Then, the estimation error can be calculated as

$$e^{U} = \frac{|\overline{l_{est}^{U}} - \overline{l_{gt}^{U}}|}{\overline{l_{gt}^{U}}}, \tag{22}$$

$$e^{W} = \frac{|\overline{l_{est}^{W}} - \overline{l_{gt}^{W}}|}{\overline{l_{gt}^{W}}}. \tag{23}$$

Table I presents mean of the estimation values based on the calibration algorithm and its deviation from mean of the Kinect captured ground truth. Overall, the average error is 4.43%.

The effect of the calibration procedure can be observed by visualizing position trajectories of the elbow joint and the wrist joint. Fig. 2 illustrates one example of the reconstructed position trajectories where the subject has performed one set of calibration motions. Fig. 2(a) plots the position trajectories in individual sensors' own temporary global reference frames while Fig. 2(b) reconstructs those in the uniform global reference frame. Both figures present a back view in the coronal plane. Fig. 2(c) presents the calibrated position trajectories in 3D space. For comparison, Fig. 2(d) plots the Kinect captured position trajectories by resetting the position of the shoulder joint to be $\mathbf{0}$ at each frame.

IV. Conclusion

This paper has introduced a simple calibration method used for upper limb motion tracking and reconstruction. Its contribution includes: 1) a global reference frame is constructed without the requirement of aligning the sensors to each other or with the arm segments; 2) position trajectories of the elbow joint and the wrist joint can be reconstructed for visualization without manually measuring the arm length; 3) sensors on the upper arm and the lower arm can be automatically differentiated without the prior knowledge of their mounting locations. Verification of the calibration algorithm based on the Kinect captured pseudo ground truth indicates error of the arm length estimation is less than 5%. Due to the simple calibration motion it requires, the calibration method is applicable to daily activity monitoring especially when feedback to users is available on whether calibration is successful.

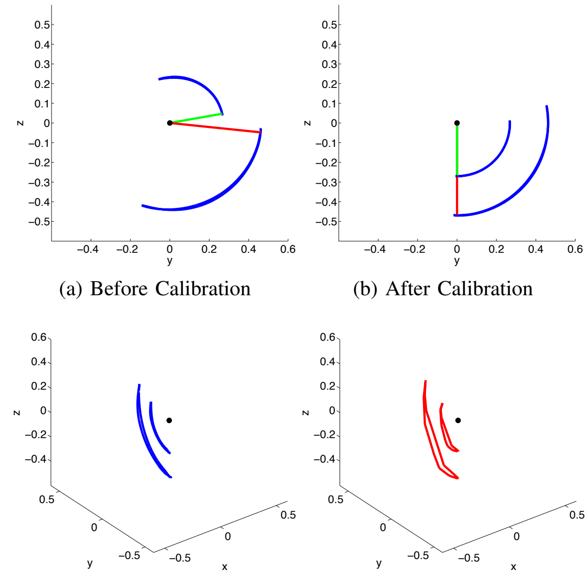

(a) Before Calibration (b) After Calibration

(c) Sensor Based Estimation (d) Kinect Based Ground Truth

Fig. 2: Position trajectories of the elbow joint and the wrist joint.

References

[1] B. Dobkin and A. Dorsch, "The promise of mhealth daily activity monitoring and outcome assessments by wearable sensors," *Neurorehabilitation and Neural Repair*, vol. 25, no. 9, pp. 788–798, 2011.

[2] R. Jafari, W. Li, R. Bajcsy, S. Glaser, and S. Sastry, "Physical activity monitoring for assisted living at home," in *4th International Workshop on Wearable and Implantable Body Sensor Networks (BSN 2007)*, vol. 13, 2007, pp. 213–219.

[3] I. Tien, S. Glaser, R. Bajcsy, D. Goodin, and M. Aminoff, "Results of using a wireless inertial measuring system to quantify gait motions in control subjects," *Information Technology in Biomedicine, IEEE Transactions on*, vol. 14, no. 4, pp. 904–915, 2010.

[4] Y. Wang, X. Xu, M. Batalin, and W. Kaiser, "Detection of upper limb activities using multimode sensor fusion," in *Biomedical Circuits and Systems Conference (BioCAS), 2011 IEEE*, 2011, pp. 436–439.

[5] M. El-Gohary, L. Holmstrom, J. Huisinga, E. King, J. McNames, and F. Horak, "Upper limb joint angle tracking with inertial sensors," in *Engineering in Medicine and Biology Society (EMBC), 2011 Annual International Conference of the IEEE*, 2011, pp. 5629–5632.

[6] C. Chien, J. Xia, O. Santana, Y. Wang, and G. Pottie, "Non-linear complementary filter based upper limb motion tracking using wearable sensors," in *Acoustics, Speech and Signal Processing (ICASSP), 2013 IEEE International Conference on*, 2013, pp. 963–967.

[7] Y. Wang, J. Xu, X. Xu, X. Wu, G. Pottie, and W. Kasier, "Inertial sensor based motion trajectory visualization and quantitative quality assessment of hemiparetic gait," in *Proceedings of the 8th International Conference on Body Area Networks*, 2013, pp. 169–172.